

# Novel Rotor Design for High-Speed Solid Rotor Induction Machines

Daniel Tunc MCGUINNESS, Mehmet Onur GULBAHCE, and Derya Ahmet KOCABAS

Dept. of Electrical Engineering, Istanbul Technical University, Istanbul, Turkey  
mcguinness@itu.edu.tr, ogulbahce@itu.edu.tr, kocabasde@itu.edu.tr

## Abstract

**Solid rotor induction motors (SRIM) became increasingly prominent in high-speed drive applications with the development of efficient power electronics systems. These types of motors are easier to manufacture compared to conventional caged rotor induction machines (CRIM). In addition to that their high material integrity and high thermal properties makes them suitable to be used for high-pressure and high-speed drive applications.**

**This paper proposes a new innovative rotor type for SRIM using in high-speed drive applications. This rotor type consists of hybrid construction of axially slitted and coated solid rotor structures and it is named as Shielded Axially Slitted Solid Rotor Induction Machine (SASSRIM) by the authors. In order to obtain performance characteristics of the novel designed rotor type, transient magnetic model is analyzed by finite element method (FEM). Finite Element Analysis (FEA) results show that rated output torque of SASSRIM is higher and more stable than other solid rotor structures. The brand new design also decreases the total losses, thereby making it more efficient than other conventional solid rotor designs.**

## 1. Introduction

This paper complements another paper by the same authors [1] where comparison of known solid rotor types for the same rated speed (slip) used in this study.

Due to its simple structure, the usability of high speed induction motors have become increasingly popular in the fields of high pressure pumps, high speed gas compression systems and in small energy compression units [2]. Structure of a conventional solid rotor consists of steel to set up both main flux-carrying parts and the shaft itself which has worse ferromagnetic properties. Due to their simple rotor structure and high thermal properties, Solid Rotor Induction Machines (SRIM) became a cheap and reliable alternative to Caged Rotor Induction Machines (CRIM) in high speed applications.

Even though their main principle operation is similar to other induction motors, considerable attention is needed for current density of rotor, temperature properties, magnetic properties and mechanical stress for a successful design [3, 4]. Although a SRIM has good mechanical and fluid dynamical properties, its electromagnetic properties are unsatisfactory. When the properties of solid rotor are questioned, its low power factor and its high time-spatial harmonic losses are prevalent.

The most common type for solid rotors is the smooth steel cylinder (SSRIM) [5]. As a result of its simple structure, it has the best mechanical, fluid and thermal dynamics than that of other rotors [6]. However, its electromagnetic properties are not

as good as other types. Its rated slip value is much higher for same output torque. Furthermore, depending on its geometrical properties, SSRIM cannot filter any of *time and spatial harmonic losses* in the air-gap. This causes high rotor losses and low efficiency. Different rotor types have been investigated in order to improve the electromagnetic and electromechanical performance, such as axially-slitted solid (ASSRIM) and coated solid rotor (CSRIM). However, their mechanical integrity is inferior to that of a SSRIM [7].

Axially slitted rotor helps to reduce the impacts of rotor losses caused by the air-gap harmonics [2]. The fundamental component of magnetic flux penetrates deeper into the rotor resulting in an improvement in the electromagnetic performance of the motor. In addition, the output torque of ASSRIM is higher than that of SSRIM [8]. This technique also reduces the rotor surface eddy current losses. However, because of the changed geometric shape of the rotor, the air-friction loss becomes more prominent at high-speed values.

Another improving method is to coat the rotor with a thin sleeve of highly conductive material together with conductive end rings on both ends. Coating material is usually chosen with high conductivity and high thermal capability [2]. The eddy currents are mainly concentrated inside the coating material [9, 10]. Coating the rotor reduces the effects of air-gap harmonics and it acts as a low-pass filter. In addition, electromagnetic performance and mechanical operational properties of motor improves. Previous studies show that coated rotor is better than previously mentioned SRIM types at high-speed operation [11].

When designing a solid rotor induction machine, the electromagnetic and mechanical properties of the rotor material must be chosen accordingly. This choice greatly affects the field distribution and the mechanical stress on rotor structure.

In this study, design of a motor having a new rotor type named as Shielded Axially Slitted Solid Rotor Induction Motor (SASSRIM) is proposed for high-speed drive applications. The new rotor type seems mainly a combination of two different conventional rotor designs. Axially slit are radially-covered by a thin layer of high-conductive coating material. Due to high-conductivity and high thermal integrity, coating material is chosen as copper. Slitted rotor material is chosen as steel-1010 depending on its availability in the market and its magnetic properties. Proposed new structure is analyzed by FEA tools for numerous speed levels in order to obtain performance characteristics, the distributions of magnetic flux and eddy current density in rotor. Only simulation results for 11300 rpm is presented to visualize one of the obtained results for the proposed design including the distributions of magnetic flux and eddy currents, and besides calculated core-loss, total loss and efficiency are given.

## 2. Loss Models Used In the Study

Losses in electrical machines can be divided into magnetic and electrical losses. All these losses are converted to heat which causes the temperature of the machine to rise. In this section, individual methods used to calculate loss portions for the novel rotor design are given below.

### 2.1. Calculation of Core Losses

Time-varying magnetic flux is main reason of core loss in ferromagnetic materials [12]. It has been accepted that the average core loss per unit volume ( $P_{Fe}$ ) are the sum of hysteresis power loss ( $P_{hys}$ ) and eddy current power loss ( $P_{eddy}$ )

$$P_{fe} = P_{hys} + P_{eddy} \quad (1)$$

Hysteresis loss is caused by the discontinuous property of the magnetization process at a very microscopic scale. This value is equal to the area of the quasi-static hysteresis loop times magnetizing frequency.

The eddy current loss can be separated into;

- Classical eddy current loss
- Anomalous eddy current loss

$$P_{eddy} = P_{classical} + P_{excess} \quad (2)$$

The classical eddy current loss is related to the macroscopic large-scale behavior of the magnetic domain structure. The anomalous loss ( $P_{excess}$ ) is caused by the domain wall motion which generates local eddy currents in the close proximity of moving walls, and by the wall interaction with the lattice inhomogeneity [13]. Accordingly, Total Core Loss can be explained in the equation given below where,  $K_h$  is the hysteresis coefficient;  $K_c$  is the classical eddy coefficient;  $K_e$  is the excess or anomalous eddy current coefficient due to magnetic domain;  $B_{max}$  is the maximum amplitude of the flux density and  $f$  is the frequency.

$$W_r = K_h B_{max}^2 f + K_c (B_{max} f)^2 + K_e (B_{max} f)^{1.5} \quad (3)$$

### 2.2. Calculation of Copper Losses

The calculation of copper losses can be calculated using classical methods. When a current flows through a conductor because of the resistivity of conductors against flowing of current, joule losses occur. While most of the losses occur in form of  $I^2R$ , some abnormal losses are caused by 1<sup>st</sup> and 2<sup>nd</sup> order of displacements. These are caused by unbalanced currents shared by parallel wires per slot and skin effect due to each wire.  $R_S$  is stator winding resistance at operating temperature,  $I$  is current flowing from stator winding,  $P_{Cu,1cd}$  is 1<sup>st</sup> order current displacement loss,  $P_{Cu,2cd}$  is 2<sup>nd</sup> order current displacement loss,  $P_{Cu,cd}$  is total current displacement losses and  $P_{CuS}$  is total copper loss occurs in stator winding. Accordingly, the equation for the total displacement loss and total copper loss occurs in stator winding given in (4) and (5).

$$P_{Cu,cd} = P_{Cu,1cd} + P_{Cu,2cd} \quad (4)$$

$$P_{CuS} = 3I^2R_S + P_{Cu,cd} \quad (5)$$

### 2.3. Calculation of Rotor Eddy-Current Losses

Rotor eddy current losses ( $P_{r,eddy}$ ) are the summation of the following values;

- Fundamental component ( $P_{r,fund}$ ) dependent on the rotor frequency
- High-frequency eddy current losses ( $P_{r,hf}$ ) caused by the slitted geometry [14].

Parameters for losses are calculated with a time-stepping FEM, using the equations written below where  $\rho$  is the specific rotor resistance of the rotor material.

$$P_{Ft,r} = \int_V \rho J_{Ft}^2 dV \quad (5)$$

$$P_{r,eddy} = P_{r,fund} + P_{r,hf} \quad (6)$$

Eddy current losses in the rotor is divided into three distinct categories. These are as follows;

- Beneath the rotor surface with a penetration depth of  $d_e$ , ( $P_{r,surface}$ )
- Loss that occurs in the teeth ( $P_{r,teeth}$ )
- Loss that occurs in the yoke ( $P_{r,yoke}$ )

With these parameters known total eddy current loss in rotor is given below;

$$P_{r,fund} = P_{r,surface} + P_{r,teeth} + P_{r,yoke} \quad (7)$$

## 3. Design of the Proposed New Rotor Type and Its Transient Magnetic Model

Due to non-linear properties of rotor material, design of solid rotor induction motor is not as easy as a conventional CRIM. After determination of main dimensions of motor, the design is aided by finite element method. Proposed new design for the study is a simple solid rotor having slits and outer layer of the slits are covered with copper. The coated copper thickness is taken 1mm in order to achieve optimal electromagnetic performance depending on related studies [15]. Slitted part is made from steel 1010. Optimal number of slits and depth of these slits are determined according to previous studies [12].

According to [16], the optimal depth of a slit needs to be half of the radius of rotor with a width of 2 mm. Mechanical stress caused by high centrifugal force does not allow deeper or wider slits. In addition to this, copper end-rings are also added to rotor ends in order to improve the electromagnetic performance of rotor. Placing copper end-rings on rotor sides induces higher electromagnetic torque at a certain slip than that of a rotor without end-rings [8]. All geometrical and electrical quantities of designed SASSRIM are given in Table 1.

**Table 1.** Parameter of newly designed SASSRIM

Symbol	Quantity	Value
P	Rated Output Power	4 kW
V/f	Rated Voltage/Frequency	380 V/200 Hz
I	Rated Current	8 A
$n_r$	Speed of rotor	11300 min <sup>-1</sup>
$Q_s$	Number of stator slot	36
$Q_r$	Number of rotor slot	28
$D_i$	Inner diameter of stator	0.08m
$D_{out}$	Outer diameter of stator	0.15m
$D_2$	Diameter of rotor	0.0794m
$L_i$	Total length of rotor	0.10m
$k_{fe}$	Stacking factor	0.94
$S_{slit}$	Number of Slits	28
$\alpha_{slit}$	Angle between two slits	12.85°
$\zeta_{slit}$	Slit length	0.1985m
$\delta_{coat}$	Width of coating material	1mm

Since a SRIM is heavily influenced by the skin effect; skin depth based mesh algorithm is used on rotor surface in order to obtain more accurate results. 2D transient magnetic model and structure of mesh are given in Fig. 1.

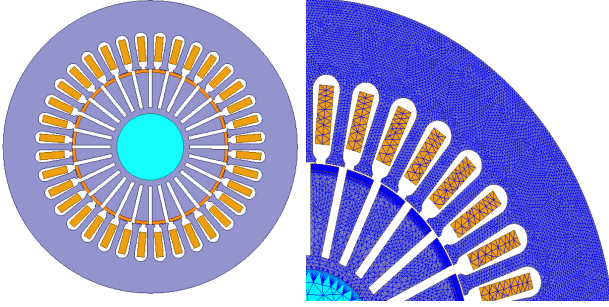


**Fig. 1.** 2D transient magnetic model of the motor having the proposed new rotor and skin depth based mesh structure

Electromagnetic performance is obtained by 2D transient magnetic model using FEM. 2D FEA can include 3D rotor end effects by increasing the rotor core resistivity [16]. Resistivity of rotor material is multiplied by end-effect factor ( $k_e$ ) which is calculated as in (8) where  $\rho_R$  is resistivity of rotor material,  $\rho_R'$  is equivalent resistivity including end-effect. (9) defines end-effect factor while introducing C coefficient depending on the type of material which is 0.3 for thick copper end-rings. The coefficient  $\alpha$  is represented in (10) where  $k_R$  is Russell factor [16],  $\tau_p$  is pole pitch in meter,  $l_{Fe}$  is active rotor length.

$$\rho_R' = k_e \cdot \rho_R \quad (8)$$

$$k_e = 1 + C \cdot (\alpha - 1) \quad (9)$$

$$\alpha = \frac{1}{k_R} = \frac{1}{1 - \frac{2 \cdot \tau_p \tanh\left(\frac{\pi l_{Fe}}{2 \tau_p}\right)}{\pi l_{Fe}}} \quad (10)$$

#### 4. FEA Results

2D transient magnetic model using FEM solves electrical and magnetic circuits at the same time for a small time step. In this

study, 10 time steps per revolution is used and spatial harmonic effects of air-gap MMF are taken into account. However, supply voltage is assumed to be pure sinusoidal and effects of time harmonics are not considered. In order to obtain torque-speed characteristics of the proposed motor, the motor is analyzed for 18 different speed levels between 0 and 12000 rpm. Magnetic flux density, magnetic flux lines and rotor current density are obtained and core-loss, total loss and efficiency are calculated for each speed level using Loss Models given in section 2.

In order to visualize the output values of the study, only results of 11300 rpm which is chosen as rated speed is given. Magnetic flux density, magnetic flux lines and rotor current density for this speed are shown in Figures 3, 4 and 5. Combined electromagnetic torque vs speed curve is given in Figure 6. Calculated values for Core, Copper and Rotor losses and efficiency are shown in Table 2. Calculated efficiency is higher than that of the motors used in [1].

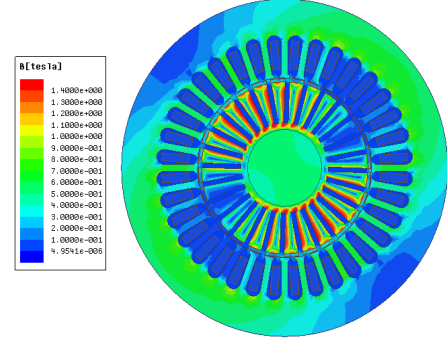


**Fig. 3.** Magnetic Flux Density of designed motor

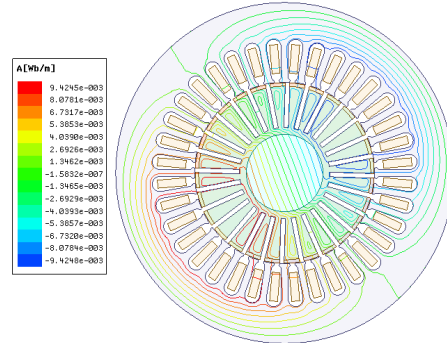


**Fig. 4.** Magnetic flux lines of designed motor

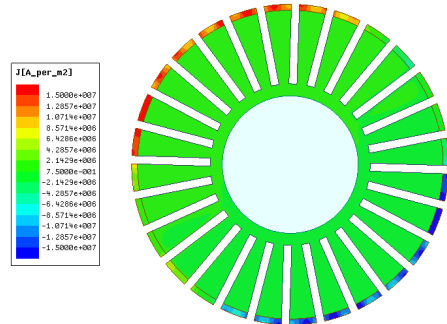


**Fig. 5.** Eddy current density distribution of proposed rotor

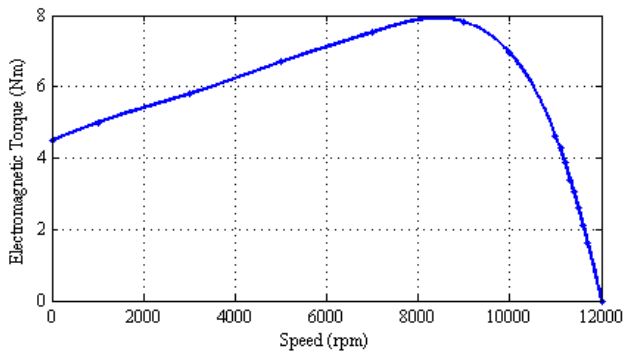


Fig. 6. Torque-Speed Characteristic of SASSRIM

Table 2. Total loss quantities of designed motor

Symbol	Quantity	Value
$P_{fe}$	Core loss	122 W
$P_{rotor}$	Rotor Loss	270 W
$P_{Cu}$	Copper loss	235 W
$P_{friction}$	Mechanical loss	55 W
$P_{totallosses}$	Total loss	682 W
$\eta$	Efficiency	85,5%

## 5. Conclusion

In this study, a new rotor type for SRIM for high-speed drive applications is proposed. The novel rotor type is mainly the hybrid of axially slitted and coated solid rotor structures and it is named as Shielded Axially-Slitted Solid Rotor Induction Machine (SASSRIM) by the authors. Designed SASSRIM is modelled in 2D transient magnetic analysis software and performance characteristics are obtained by using FEM. FEA results show that rated output torque of SASSRIM is higher and smoother than other solid rotor types in [1]. The proposed structure also has decreased total losses, thereby making it more efficient than other solid rotor designs [1]. Adverse mechanical effects and torque ripple caused by spatial harmonics is reduced by SASSRIM. In addition to that, axially-slitted rotor increases the tangential flux component which penetrates in rotor body. The deeper magnetic flux raises the induced eddy currents on rotor resulting more electromagnetic torque production. However, deeper flux penetration increases the core loss of rotor mass.

## 5. References

[1] D. T. McGuinness, M. O. Gulbahce, D. A. Kocabas, "Performance Comparison of Different Rotor Types for High-Speed Induction Motors", 9th International Conference on Electrical and Electronics Engineering (ELECO), 2015

[2] Aho, T.; Sihvo, V.; Nerg, J.; Pyrhonen, J., "Rotor Materials for Medium-Speed Solid-Rotor Induction Motors", Electric Machines & Drives Conference, 2007 IEEE International, vol.1, no., pp.525-530, 3-5 May 2007 doi: 10.1109/IEMDC.2007.382722

[3] Papini, L.; Gerada, C., "Thermal-electromagnetic analysis of solid rotor induction machine", 7th IET International Conference on Power Electronics, Machines and Drives (PEMD 2014), pp.1-6, 8-10 April 2014 doi: 10.1049/cp.2014.0462

[4] Gerada, D.; Mebarki, A.; Brown, N.L.; Bradley, K.J.; Gerada, C., "Design Aspects of High-Speed High-Power Density Laminated-Rotor Induction Machines", IEEE Transactions on Industrial Electronics, vol.58, no.9, pp.4039-4047, Sept. 2011 doi: 10.1109/TIE.2010.2098364

[5] Juha Pyrhonen, Tapani Jokinen, Valeria Hrabovcova "Design of Rotating Electrical Machines", February 2009, Wiley, ISBN: 978-0-470-74008-8

[6] Hamid A. Toliyat, Gerald B. Kliman, "Handbook of Electric Motors", April 22, 2004, CRC Press, ISBN 9780824741051 - CAT# DK1321

[7] L. Papini, C. Gerada, D. Gerada, Abdeslam Mebarki, "High Speed Solid Rotor Induction Machine: Analysis", 2014 17th International Conference on Electrical Machines and Systems (ICEMS), Oct. 22-25, 2014, Hangzhou, China

[8] Klíma, J.; Vitek, O., "Analysis of high-speed induction motor," 2014 16th International Conference on Mechatronics - Mechatronika (ME), pp.85-91, 3-5 Dec. 2014 doi: 10.1109/MECHATRONIKA.2014.7018240

[9] J. Gieras and J. Saari, "Performance calculation for a high speed solid rotor induction motor", Industry Applications, IEEE Transactions on, vol. 59, no. 6, pp. 2689-2700, 2012.

[10] Shah, M.R.; Sang-Bin Lee, "Optimization of Shield Thickness of Finite-Length Solid Rotors for Eddy-Current Loss Minimization", Industry Applications, IEEE Transactions on, vol.45, no.6, pp.1947,1953, Nov.-dec.2009

[11] Aho, T.; Nerg, J.; Pyrhonen, J., "Analysing the effect of the rotor coating on the rotor losses of medium-speed solid-rotor induction motor", International Symposium on Power Electronics, Electrical Drives, Automation and Motion (SPEEDAM 2006), pp.103-107, 23-26 May 2006 doi: 10.1109/SPEEDAM.2006.1649752

[12] J. HUPPUNEN, High-speed solid-rotor induction machine: electromagnetic calculation and design. Lappeenranta: Lappeenranta Teknillinen Yliopisto, 2004. ISBN 95-176-4981-9.

[13] J. Saitz, "Calculation of Iron losses in Electrical Machines", Helsinki University of Technology, Laboratory of Electromechanics, Report 51, Espoo, 1997, 57 p. ISBN 951-22-3503-X

[14] S. L. Ho, W. N. Fu and H. C. Wong: "Estimation of Stray Losses of Skewed Rotor Induction Motors Using Coupled 2-D and 3-D Time Stepping Finite Element Methods", IEEE Trans. Map, vol.34, No.5, 3102, 1998

[15] K. Tatis, A. Kladas And J.Tegopoulos, "Solid Rotor Induction Machine Optimisation based on Finite Element Techniques"

[16] Mekuria, "Development of a high speed solid rotor asynchronous drive fed by a frequency converter system" PhD Thesis, 2013, Technical University of Darmstadt, Germany

[17] Aho, T.; Nerg, J.; Pyrhonen, J., "Experimental and Finite Element Analysis of Solid Rotor End Effects," International Symposium on Industrial Electronics, 2007. ISIE 2007. IEEE, vol., no., pp.1242-1247, 4-7 June 2007 doi: 10.1109/ISIE.2007.4374776

- [18] Katsumi Yamazaki , Member, IEEE ,”Harmonic Copper and Iron Losses Calculation of Induction Motor Using Nonlinear Time-Stepping Finite Element Method “,*IEEE, 2001*